

RESEARCH

Open Access



# Systemic necrosis induced by overexpression of wheat yellow mosaic virus 14K suppresses the replication of other viruses in *Nicotiana benthamiana*

Yan Zhang, Chuanxi Zhang, Junmin Li, Jianping Chen\* and Gang Lu\*

## Abstract

Systemic necrosis, induced by plant virus-derived elicitors, is considered as one of the most severe symptoms. It has never been reported that the elicitors encoded by wheat yellow mosaic virus (WYMV) can induce systemic necrosis in plant. In this study, we discovered that the WYMV-encoded 14K protein localized to the endoplasmic reticulum (ER) membrane and triggered a necrotic symptom in *Nicotiana benthamiana* at 5 days post-infiltration (dpi). Meanwhile, overexpression of WYMV 14K suppressed the replication of tobacco rattle virus (TRV) and potato virus X (PVX). Additionally, deletion of the transmembrane domain and substitution of two non-conserved regions in 14K resulted in the loss of the ability of this protein to induce systemic necrosis. Moreover, the 14K homologous proteins of other bymoviruses failed to induce systemic necrosis. Our results, for the first time, reveal that WYMV 14K induces systemic necrosis and suppresses the replication of other viruses.

**Keywords:** Systemic necrosis, Wheat yellow mosaic virus, 14K protein, Virus infection, Elicitor

## Background

Wheat yellow mosaic virus (WYMV), which belongs to the genus *Bymovirus* in the family *Potyviridae*, is an important wheat virus that causes serious crop yield losses in East Asia (Han et al. 2000). WYMV can be transmitted by plasmodiophorid *Polymyxa graminis*, and the symptoms of WYMV infection in host wheat include yellow-striped leaves, anthocyanin accumulation, stunted growth and dwarfism (Takeuchi et al. 2010).

WYMV virions are flexuous filaments with two modal lengths (about 275 and 550 nm) and a diameter of 13 nm. The genome of WYMV comprises two

linear, positive-sense and single-stranded RNAs, RNA1 and RNA2 (Li et al. 1999; Li and Shirako 2015). RNA1 comprises 7635 nucleotides and encodes a large polyprotein that is proteolytically processed to generate eight mature proteins, including P3, 7K, cylindrical inclusion (CI), 14K, viral genome-linked protein (VPg), nuclear inclusion a protease (NIa-Pro), nuclear inclusion b (NIb) and a coat protein (CP). In addition, a small open reading frame (ORF) P3N-PIPO protein can be generated by frameshift mutation in P3 (Chung et al. 2008; Wei et al. 2010). WYMV RNA2 (3650 nucleotides in length) encodes a polyprotein that contains P1 and P2 (Namba et al. 1998). Among these proteins, 14K, corresponding to the 6K2 protein of other potyviruses, is a small protein rich in hydrophobic amino acids and has a transmembrane (TM) domain. Notably, the 6K2 protein plays an important role in viral replication, intercellular movement, and reorganization of endoplasmic reticulum (ER) membrane to establish a systemic

\*Correspondence: jianpingchen@nbu.edu.cn; lugang@nbu.edu.cn  
State Key Laboratory for Managing Biotic and Chemical Threats to the Quality and Safety of Agro-Products, Key Laboratory of Biotechnology in Plant Protection of Ministry of Agriculture and Zhejiang Province, Institute of Plant Virology, Ningbo University, Ningbo 315211, China



infection on host plants (Wei and Wang 2008; Cotton et al. 2010; Jiang et al. 2015). However, the function of WYMV-encoded 14K protein in viral infection remains unknown.

Virus infection of host plants induces a variety of symptoms, among which systemic necrosis is recognized as one of the most severe symptoms leading to cell death. Typically, systemic necrosis starts from the virus-infected leaves and expands along the vascular system to the systemic leaves (Kim et al. 2008). Since the virus-infected tissues are accompanied by the localized necrotic lesions that eventually lead to cell death, the necrotic response is considered as a defense signal of host plant in response to virus infection. Hypersensitive response (HR), a type of programmed cell death associated with plant resistance to viruses, has been shown to share similar physiological and biochemical features with systemic necrosis (Kim et al. 2008; Komatsu et al. 2011; Aguilar et al. 2015). HR shows generally localized cell death within the infected areas upon the recognition of a virus-encoded elicitor protein by the respective plant resistance protein (R protein) complex (Soosaar et al. 2005). Several plant virus-encoded elicitor proteins, including the P25 pathogenicity factor of potato virus X (PVX) (Aguilar et al. 2015; Yang et al. 2020), the TuNI protein of turnip mosaic virus (TuMV) (Kim et al. 2010), the polymerase protein of plantago asiatica mosaic virus (PLAMV) (Komatsu et al. 2011) and the movement protein P11 of garlic virus X (GarVX) (Lu et al. 2016), have been found to trigger systemic necrosis through interfering with protein synthesis and disrupting cellular balance in host plants. However, it remains unclear whether WYMV also encodes similar elicitors to induce systemic necrosis.

In this study, we identified one of the possible but crucial functions of WYMV-encoded 14K protein in triggering plant systemic necrosis in *Nicotiana benthamiana*. As discovered using the recombinant TRV- and PVX-mediated overexpression system, 14K-induced necrosis affected the systemic infection of these two viruses, and the frameshift mutation of 14K led to loss of function of the protein in inducing systemic necrosis at 5 dpi. Additionally, the TM domain and two non-conserved regions in 14K were shown to be critical for inducing systemic necrosis. Moreover, the 14K homologous proteins from other bymoviruses failed to induce systemic necrosis. These results show that WYMV 14K can induce systemic necrosis and suppress the replication of other viruses in *N. benthamiana*.

## Results

### Systemic necrosis is induced by a WYMV peptide in *N. benthamiana*

To investigate whether systemic necrosis was induced by the WYMV-derived peptides, we divided the genome sequences (RNA1 and RNA2) of WYMV into 18 and 9 fragments (500–600 bp per fragment), respectively, and

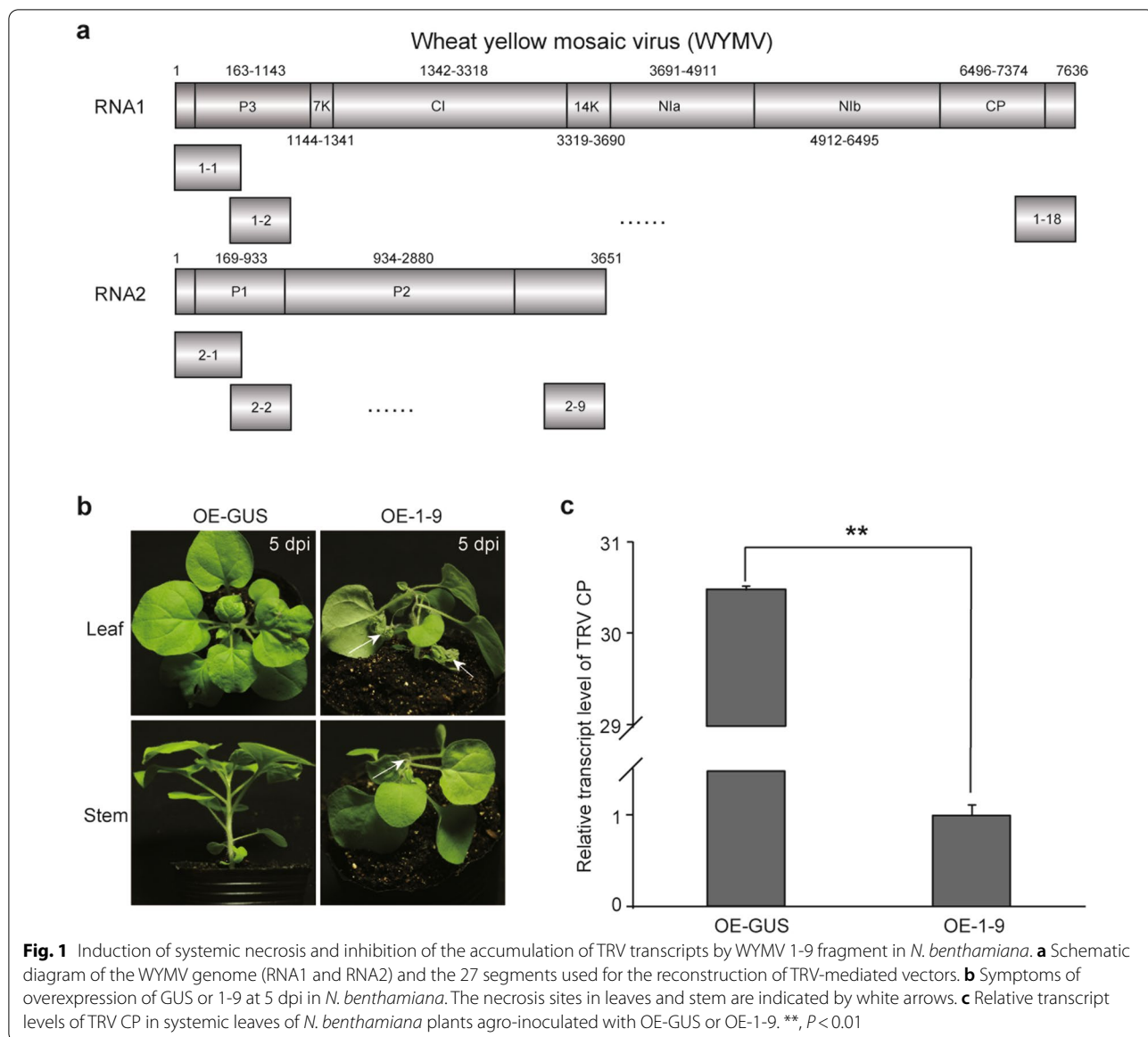
cloned them individually into the tobacco rattle virus (TRV)-mediated overexpression (OE) vector (Fig. 1a). After each of the WYMV genomic fragments was agro-inoculated into *N. benthamiana* leaves, only the 1-9 fragment (OE-1-9)-inoculated leaves exhibited severe necrosis symptom at 5 dpi, while leaves inoculated with other fragments and control (overexpression of  $\beta$ -glucuronidase, short for OE-GUS) showed no necrosis symptom at 5 dpi (Fig. 1b). In systemically infected leaves, the accumulated TRV CP in OE-1-9-inoculated plants was much lower than that in OE-GUS-inoculated plants (Fig. 1c).

### WYMV 14K protein triggers systemic necrosis and inhibits systemic infection of other viruses in *N. benthamiana*

Next, to explore the 1-9 fragment-induced necrosis symptom, we divided this fragment into seven parts based on the presence of seven start codons (from 1-9M1 to 1-9M7), which were then individually cloned into the TRV overexpression vector (Fig. 2a) and agro-inoculated into *N. benthamiana*. At 5 dpi, necrosis symptom was exhibited in leaves inoculated with 1-9M1, but not in leaves inoculated with the others and the control (Fig. 2b). When analyzing the 1-9M1 sequence, we found that it contained a complete sequence of WYMV 14K (Additional file 1: Table S1) and wondered whether 14K could induce systemic necrosis. Thereafter, the 14K sequence was over-expressed (OE-14K) in *N. benthamiana* via the TRV-mediated system and systemic necrosis symptom was observed at 5 dpi (Fig. 2c). Also, in the non-inoculated systemic leaves, the transcript level of TRV CP in OE-14K-inoculated plants was significantly down-regulated by up to 30 times compared with that in OE-GUS-inoculated plants (Fig. 2d). Similarly, when the PVX-mediated overexpression vector was used, PVX-14K-inoculated leaves exhibited significantly inhibited accumulation of PVX CP compared with PVX-GUS inoculated plants at 5 dpi (Additional file 2: Figure S1).

Western blotting analysis was then carried out to verify the accumulation of 14K protein in inoculated leaves. As shown in Fig. 2e, 14K protein was present in leaves agro-infiltrated with OE-14K at 2 dpi. Meanwhile, to determine the subcellular localization of 14K protein, we transiently expressed the recombinant 14K-GFP in *N. benthamiana* leaves using agro-infiltration. It was found that 14K-GFP was co-localized with the endoplasmic reticulum (ER) marker mCherry-HDEL under the confocal laser scanning microscopy (Fig. 2f).

Additionally, frameshift mutation of 14K was used to further confirm that the systemic necrosis symptom was induced by the 14K protein but not by the other WYMV-encoded proteins. After deletion of either the 13th base (T) or the 14th base (T), or simultaneous deletion of



both of these two bases in the 14K sequence, the protein sequence is changed, and the resultant two mutants of 14K, 14K-FM ( $\Delta T$ ) and 14K-FM ( $\Delta TT$ ), were overexpressed to observe if they could induce necrosis symptom (Fig. 3a). The results showed that both of these two

mutants lost the ability to induce systemic necrosis at 5 dpi in *N. benthamiana* (Fig. 3b), suggesting that the WYMV-encoded 14K protein induced systemic necrosis in *N. benthamiana*. In addition, when the other eight viral proteins encoded by the WYMV genome were

(See figure on next page.)

**Fig. 2** WYMV 14K protein triggers systemic necrosis and inhibits TRV systemic infection in *N. benthamiana*. **a** Schematic diagram of the positions of 1-9 deletion mutations and 14K sequences corresponding to the WYMV genome. **b** Symptoms of overexpression of WYMV 1-9 mutants in *N. benthamiana* at 5 dpi. OE-GUS was used as a negative control. The necrosis sites in leaves are indicated by white arrows. **c** Symptoms of overexpression of GUS or 14K at 5 dpi in *N. benthamiana*. The necrosis sites in leaves and stem are indicated by white arrows. **d** Relative transcript levels of TRV CP in systemic leaves of *N. benthamiana* plants agro-inoculated with OE-GUS or OE-14K. \*\*,  $P < 0.01$ . **e** Detection of the expression of OE-GUS and OE-14K in infiltrated leaves through immunoblotting. The positions of expected protein bands are indicated with black arrows and Ponceau S staining showed equal loading. **f** Co-localization of 14K-GFP with the ER marker (mCherry-HDEL) at 48 hpi. Bar, 25  $\mu$ m

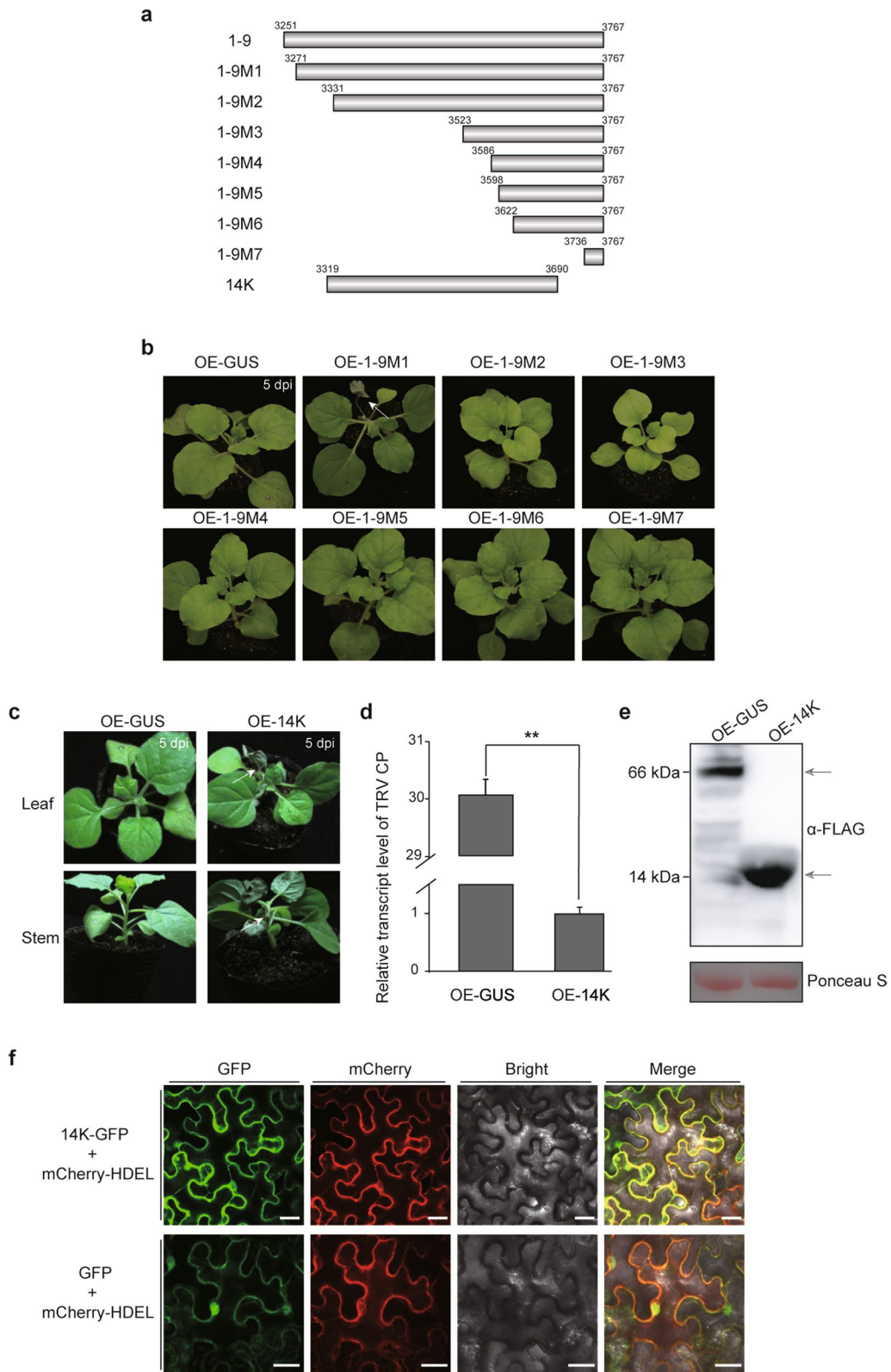


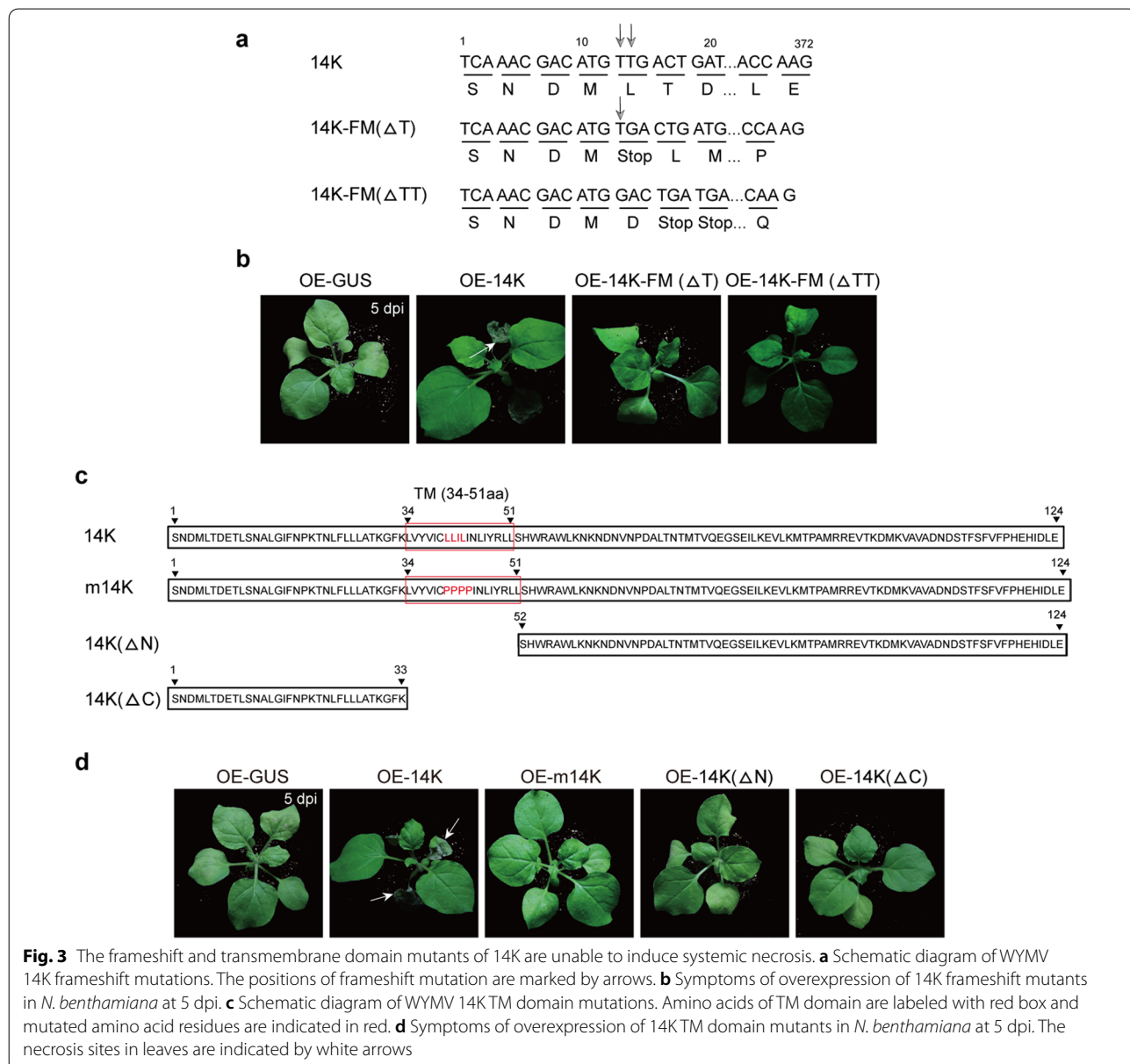
**Fig. 2** (See legend on previous page.)

overexpressed, none of them was able to induce systemic necrosis in *N. benthamiana* at 5 dpi (Additional file 2: Figure S2).

**14K transmembrane domain is critical for inducing systemic necrosis**

Based on the result that 14K protein induced systemic necrosis, we next figured out which functional domain(s) participated in the induction of systemic necrosis. Analyses of 14K sequence using multiple programs suggested that, one TM domain (34–51aa) existed in the 14K amino acid sequence (Fig. 3c). To explore whether this TM domain was involved in the function of 14K to

induce systemic necrosis, we replaced the four hydrophobic amino acids (LLIL) with prolines in the 14K TM domain and constructed the corresponding TRV-m14K overexpression vector (OE-m14K). Meanwhile, we also deleted the N-terminus and C-terminus containing the TM domain to construct the OE-14K ( $\Delta$ N) and OE-14K ( $\Delta$ C) mutants, respectively (Fig. 3c). As observed in Fig. 3d, OE-m14K, OE-14K ( $\Delta$ N) and OE-14K ( $\Delta$ C) were similar to the OE-GUS, with no obvious necrosis symptom compared with the wild-type 14K at 5 dpi. Therefore, we confirmed that the TM domain in 14K protein is indispensable for the 14K-induced systemic necrosis.



**Two non-conserved regions in 14K are required for the induction of systemic necrosis**

In addition to the TM region, we explored whether other regions were also involved in the 14K-induced systemic necrosis. Therefore, we first collected 14K sequences from five WYMV isolates (JS-BY1, JS-YC1, JS-XH3, SD-QD1 and SD-QF1) at the National Center of Biotechnology Information (NCBI) and performed alignment analysis with the isolate JS-GY1 kept in our lab. As a result, two regions (regions 1 and 2) exhibited great variability in amino acid sequence (Fig. 4a). Then, the amino acids in these two regions of 14K of JS-GY1 were

respectively replaced with those of the above-mentioned five isolates. After overexpression of these mutants in *N. benthamiana* at 5 dpi, none of the mutations in 14K induced systemic necrosis (Fig. 4b), indicating that the two non-conserved amino acid regions might be involved in the 14K-induced systemic necrosis.

**The 14K homologues from other bymoviruses failed to induce systemic necrosis**

Further, to elucidate whether the 14K proteins of other bymoviruses also induced necrosis, the 14K homologous sequences from four viruses (barley mild mosaic virus,

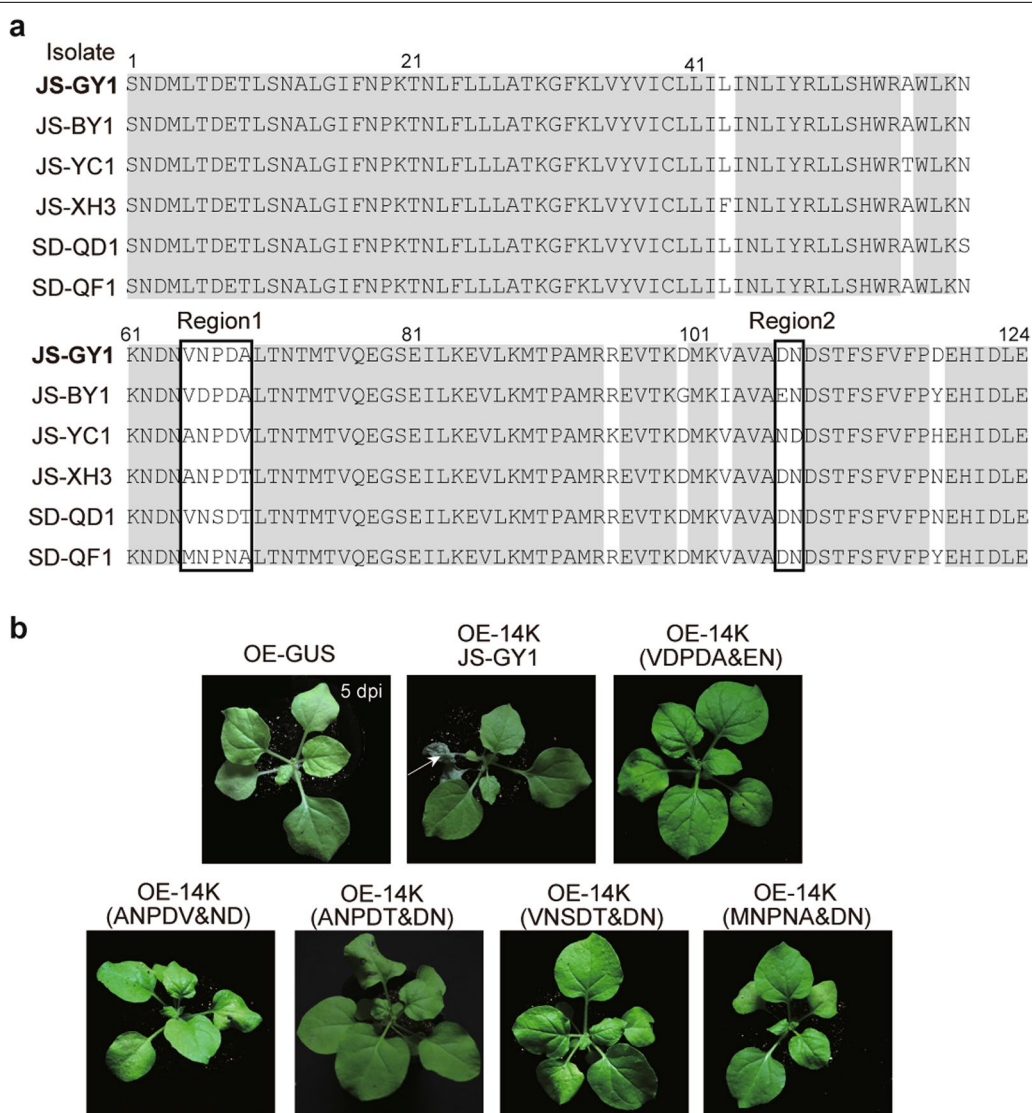


**Fig. 4** Two non-conserved regions in 14K are required for the induction of systemic necrosis. **a** Alignment analysis of 14K sequences from different WYMV isolates. Names and GenBank accession numbers of these isolates are as follows: JS-GY1 (MG678164.1), JS-BY1 (MG678162.1), JS-YC1 (MG678163.1), JS-XH3 (MG678168.1), SD-QD1 (MG678180.1) and SD-QF1 (MG678176.1). The replaced regions are indicated by black boxes. **b** Symptoms of overexpression of replaced 14K mutants in *N. benthamiana* at 5 dpi. The necrosis sites in leaves are indicated by white arrows

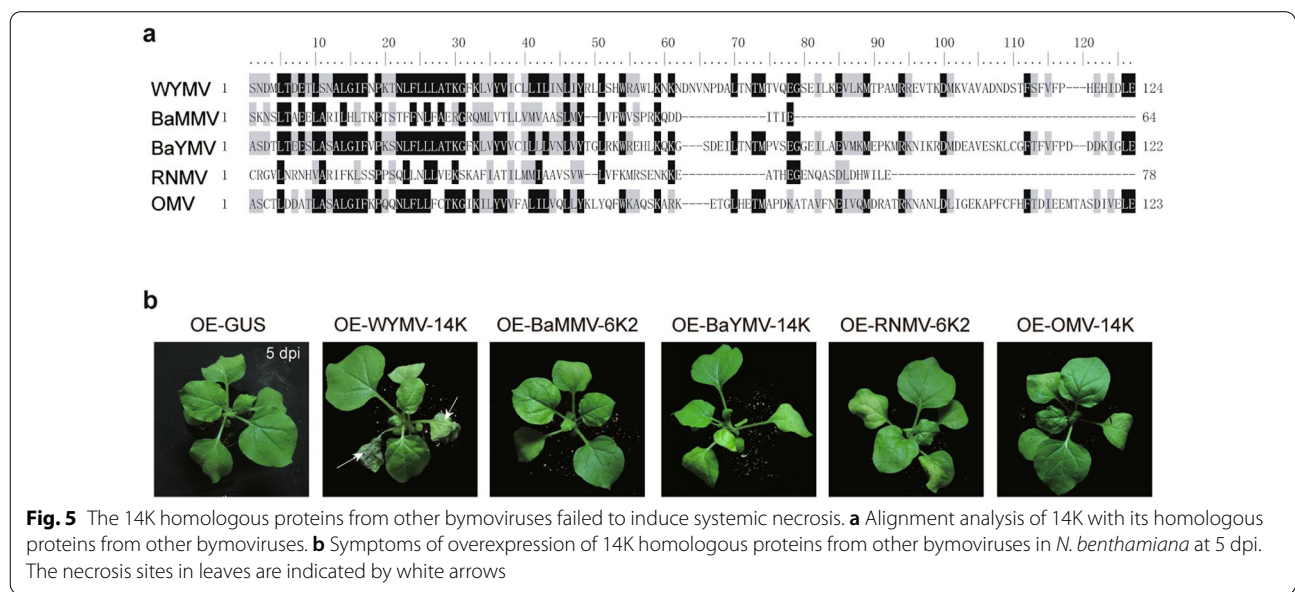
BaMMV; barley yellow mosaic virus, BaYMV; rice necrosis mosaic virus, RNMV and oat mosaic virus, OMV) were aligned with that of WYMV. It was shown that they shared 12.9–53.6% identity in amino acid sequence (Fig. 5a). Next, the 14K homologous sequences from these four viruses were individually cloned into the TRV overexpression system and infiltrated into leaves of *N. benthamiana* to detect necrosis symptom. Unlike leaves inoculated with OE-WYMV-14K, those inoculated with other four 14K homologous proteins exhibited no necrosis at 5 dpi (Fig. 5b). This result was evidenced by the finding that only WYMV-encoded 14K protein might specifically induce systemic necrosis, while other bymovirus-encoded 14K homologous proteins failed to induce systemic necrosis.

**Discussion**

Plant virus-induced systemic necrosis has been widely concerned over the past three decades and the mechanism underlying this phenomenon has been reported to be caused by a variety of factors, including systemic acquired resistance (Ward et al. 1991; Fodor et al. 1997), posttranscriptional gene silencing (van et al. 2002; Zhan et al. 2018), programmed cell death (Mittler et al. 1998; Komatsu et al. 2010; Lu et al. 2016), phloem blocking (Yoshikawa et al. 2006) and other abiotic factors (Shevchenko et al. 2004, 2007). In this study, we clarified a relationship between necrosis symptom and systemic viral infection. Using the recombinant virus vector (TRV/PVX)-mediated overexpression system, we identified that the WYMV-encoded 14K protein acted as an elicitor to induce systemic necrosis and inhibit subsequent systemic

infection of other unrelated viruses. Moreover, the sub-cellular localization of 14K protein was found to be co-localized with an ER marker, suggesting that 14K-induced necrosis response may be caused by ER stress.

By analyzing the segmentation of the WYMV genome and frameshift mutants, we confirmed that the intact 14K protein, but not other viral proteins, induced systemic necrosis in *N. benthamiana* (Fig. 2b, f). Similar necrosis symptoms have also been reported in other viruses. For instance, TuMV-encoded TuNI induces venial necrosis and forms the HR-like cell death in virus infection areas in *Arabidopsis thaliana*. This symptom is accompanied by the production of hydrogen peroxide, accumulation of salicylic acid, emission of ethylene, and subsequent expression of defense-related genes (Kim et al. 2008). Additionally, PIAMV induces necrosis response in a polymerase protein dose-dependent manner, and this response is composed of programmed cell death and inhibition of virus multiplication (Komatsu et al. 2010, 2011). Another precise mechanism suggests that HR and systemic necrosis are dependent on R protein-elicitor interaction. Previous studies have reported that HR mediated by several R proteins (N, RCY1 and Nb) can effectively inhibit the systemic movement of multiple viruses (Malcuit et al. 1999; Dinesh-Kumar et al. 2000; Sekine et al. 2006). During the systemic infection process of TRV or PVX, 14K protein localized to the ER membrane, triggered necrosis and suppressed systemic virus infection. Based on these results, we suppose that 14K-induced necrosis response may be caused by ER stress and the potential mechanism needs to be further explored.



Based on the findings that TM domain and two non-conserved regions of 14K are critical for the induction of systemic necrosis, we suggested that 14K might stimulate host endomembrane system and trigger systemic necrosis. PVX-encoded P25 protein is reported to be necessary in remodeling plant endomembranes, i.e. ER and Golgi, and in recruiting other viral proteins to form viral replication and movement complexes (Tilsner et al. 2012; Yan et al. 2012). Moreover, P25 also induces ER stress and up-regulates the expression of several ER-related genes (Aguilar et al. 2015). In addition, overexpression of garlic virus X-encoded P11 protein induces ER stress, and two TM domains of P11 are required for inducing necrosis (Lu et al. 2016). Besides, the 14K homologue 6K2 protein of potyviruses has been reported to be involved in the formation of viral replication complexes (VRCs) (Spetz and Valkonen 2004). VRCs of the genus *Potyvirus* are initially formed in ER, in which individual VRC vesicles are transported to the chloroplast via the in vivo transport pathway (Wei and Wang 2008; Wei et al. 2013). Even in the absence of viral infection, the 6K2 protein can induce vesicle formation on the ER membrane. Deletion of the hydrophobic domain of the tobacco etch virus (TEV) 6K2 results in loss of function to form the vesicle structure (Schaad et al. 1997). Therefore, we speculated that the TM domain of 14K may contribute to the formation of VRCs in ER membrane and the induction of systemic necrosis.

In summary, we identified the function of WYMV-encoded 14K protein in triggering ER-stress induced plant systemic necrosis and affecting systemic infection of other two viruses (TRV and PVX) in *N. benthamiana*. TM domain and two non-conserved regions in 14K were critical for the induction of systemic necrosis. In addition, the 14K homologous proteins from other bymoviruses failed to induce systemic necrosis. These results provide new potential strategies that contribute to the control of wheat soil-borne virus disease by the production of resistant plant materials targeting the critical viral proteins.

## Conclusions

WYMV-encoded 14K protein was identified as an elicitor that targets to the ER membrane and triggers plant systemic necrosis. Overexpression of 14K suppressed systemic infection of TRV or PVX in *N. benthamiana*. Furthermore, frameshift mutation of 14K, deletion of TM domain or two non-conserved regions in 14K led to the loss of the ability of this protein to induce systemic necrosis in *N. benthamiana*. Additionally, the 14K homologous proteins from other bymoviruses failed to induce systemic necrosis. Our study reveals for the first time that

WYMV-encoded protein can induce systemic necrosis, which broadens our knowledge on virus-induced systemic necrosis.

## Methods

### Plant materials

Wheat samples infected with WYMV were collected from a field in Gaoyou, Jiangsu Province, China (isolate JS-GY1) and stored at  $-80^{\circ}\text{C}$ . *N. benthamiana* plants were grown in a greenhouse at  $24^{\circ}\text{C}$  under a photoperiod of 16-h light/8-h dark.

### Construction of plasmids

To construct the fusion plasmids, the TRV plasmids were digested with *Pst*I at  $37^{\circ}\text{C}$  for 30 min, then, sensitive alkaline phosphatase (Thermo Fisher, USA) was added and incubated for additional 30 min to prevent self-ligation at  $37^{\circ}\text{C}$ . The PVX plasmids were digested with *Cla*I and *Sal*I at  $37^{\circ}\text{C}$  for 2 h. DNA products corresponding to the WYMV-encoded proteins were amplified by PCR and then cloned into the digested plasmids by homologous recombination technology. Positive clones were later selected and verified by Sanger sequencing analysis.

### Agroinfiltration

For *Agrobacterium*-mediated transformation of *N. benthamiana*, the recombinant expression plasmid was transformed into GV3101, which contained a helper plasmid pSoup. Thereafter, positive clones were selected and verified by Sanger sequencing. After collecting the bacteria, the bacterial precipitate was resuspended with infiltration buffer (10 mM MES, 10 mM MgCl<sub>2</sub> and 200  $\mu\text{M}$  Acetosyringone) to an optical density of 0.5 at 600 nm. The suspensions were then infiltrated into *N. benthamiana* plants.

### Subcellular localization

To detect the subcellular localization of 14K, fluorescence images were captured with an inverted Leica TCS SP8 FALCON. The GFP fluorescence was visualized using an excitation wavelength of 488 nm and emission wavelengths in the range of 500–540 nm. The mCherry fluorescence was visualized with an excitation wavelength of 561 nm and emission wavelengths in the range of 585–620 nm. Images were processed using Leica LAS X Small 3.3.0 and Adobe Illustrator CC 2021 (version 26.0).

### Western blotting

Protein samples were extracted from *N. benthamiana* using protein lysis buffer [50 mM Tris (pH=7.4), 150 mM NaCl, 1% NP-40 and 0.1% SDS] and separated by 10% SDS-PAGE, followed by transfer to a PVDF

membrane. The antigens on the membrane were detected with a monoclonal antibody conjugated with horseradish peroxidase (HRP) against Flag tag (1:10,000 dilution; Sigma). The blot was visualized with the Super ECL plus (S6009, US EVERBRIGHT) and imaged with the Luminescent Image Analyzer AI680 (GE, Sweden).

### Quantitative real-time PCR

Total RNAs were extracted from *N. benthamiana* using TRIzol reagent (Invitrogen, USA) according to the manufacturer's protocols, and then cDNA was synthesized using the HiScript II Reverse Transcriptase (Vazyme, China). Later, quantitative real-time PCR (qPCR) was performed on a LightCycler Real-Time PCR System (Roche, Swiss) with the Hieff<sup>TM</sup> qPCR SYBR Green Master Mix (Yeasen, China). The relative abundance of viral RNA in *N. benthamiana* was calculated using the  $2^{-\Delta\Delta Ct}$  method, and the expression level of housekeeping ubiquitin conjugating enzyme 2 gene (*UBC*) served as an internal reference. Three independent assays were performed, with five plants per treatment. Primers used in this study were listed in Additional file 1: Table S2.

### Virus sequence analysis

Searches for conserved domains within the genome of WYMV were performed with the Conserved Domain Database at NCBI and InterProScan program (Quevillon et al. 2005). To predict the TM domain, TMHMM 2.0 server and TMPred program were adopted (Cuthbertson et al. 2005).

### Statistical analysis

SPSS 13.0 software was used for all statistical analyses and all sample data were evaluated as standard error of the mean from three independent biological replicates. The figures were generated using Adobe Illustrator CC 2021 (version 26.0).

### Abbreviations

BaMMV: Barley mild mosaic virus; BaYMV: Barley yellow mosaic virus; CI: Cylindrical inclusion; CP: Coat protein; dpi: Days post-infiltration; ER: Endoplasmic reticulum; FM: Frameshift mutation; GarVX: Garlic virus X; Gus:  $\beta$ -Glucuronidase; HR: Hypersensitive response; JS-BY1: Jiangsu-Baoying1; JS-GY1: Jiangsu-Gaoyou1; JS-XH3: Jiangsu-Xinghua1; JS-YC1: Jiangsu-Yancheng1; Nla-Pro: Nuclear inclusion a protease; Nlb: Nuclear inclusion b; OE: Overexpression; OMV: Oat mosaic virus; ORF: Open reading frame; PIAMV: Plantago asiatica mosaic virus; PVX: Potato virus X; qPCR: Quantitative real-time PCR; R protein: Resistance protein; RNMV: Rice necrosis mosaic virus; SD-QD1: Shandong-Qingdao1; SD-QF1: Shandong-Qufu1; TEV: Tobacco etch virus; TM: Transmembrane; TRV: Tobacco rattle virus; TuMV: Turnip mosaic virus; UBC: Ubiquitin conjugating enzyme 2; VPg: Viral genome-linked protein; VRCs: Viral replication complexes; WYMV: Wheat yellow mosaic virus.

## Supplementary Information

The online version contains supplementary material available at <https://doi.org/10.1186/s42483-022-00122-4>.

**Additional file 1: Table S1.** The complete nucleotide sequence of wheat yellow mosaic virus RNA 1. The nucleotide sequence of 14K is underlined and indicated in red; **Table S2.** Primers used in this study.

**Additional file 2: Figure S1.** WYMV 14K protein triggers systemic necrosis and inhibits PVX systemic infection in *N. benthamiana*. **a** Symptoms of overexpression of PVX-GUS or PVX-14K in *N. benthamiana* at 5 dpi. The necrosis sites in leaves and stem are indicated by white arrows. **b** Relative transcript levels of PVX CP in systemic leaves agro-inoculated with PVX-GUS or PVX-14K. \*\*,  $P < 0.01$ . **Figure S2.** Other proteins encoded by WYMV are unable to induce systemic necrosis. Symptoms of overexpression of GUS and WYMV-encoded proteins in *N. benthamiana* at 5 dpi. The positions of necrosis in leaves and stem are indicated by white arrows.

### Acknowledgements

Not applicable.

### Author contributions

YZ performed the experiments and wrote the manuscript. YZ and GL analyzed the data. YZ, CZ and JL prepared the figures and tables. JL, JC and GL helped to design the experiments and revised the manuscript. All authors read and approved the final manuscript.

### Funding

This work was supported by the China Agriculture Research System from the Ministry of Agriculture of China (CARS-03-31) and the Natural Science Foundation of Ningbo City (2019A610404).

### Availability of data and materials

Not applicable.

### Declarations

### Ethics approval and consent to participate

Not applicable.

### Consent for publication

Not applicable.

### Competing interests

The authors declare that they have no competing interests.

Received: 5 February 2022 Accepted: 20 April 2022

Published online: 12 May 2022

### References

- Aguilar E, Almendral D, Allende L, Pacheco R, Chung BN, Canto T, et al. The P25 protein of potato virus X (PVX) is the main pathogenicity determinant responsible for systemic necrosis in PVX-associated synergisms. *J Virol.* 2015;89(4):2090–103. <https://doi.org/10.1128/JVI.02896-14>.
- Chung BYW, Miller WA, Atkins JF, Firth AE. An overlapping essential gene in the Potyviridae. *Proc Natl Acad Sci USA.* 2008;105(15):5897–902. <https://doi.org/10.1073/pnas.0800468105>.
- Cotton S, Grangeon R, Thivierge K, Mathieu I, Ide C, Wei TY, et al. Turnip mosaic virus RNA replication complex vesicles are mobile, align with microfilaments, and are each derived from a single viral genome. *J Virol.* 2010;83(20):10460–71. <https://doi.org/10.1128/JVI.00819-09/JVI.00819-09>.
- Cuthbertson JM, Doyle DA, Sansom MSP. Transmembrane helix prediction: a comparative evaluation and analysis. *Protein Eng Des Sel.* 2005;18(6):295–308. <https://doi.org/10.1093/protein/gzi032>.

- Dinesh-Kumar SP, Tham WH, Baker BJ. Structure–function analysis of the tobacco mosaic virus resistance gene N. *Proc Natl Acad Sci USA*. 2000;97(26):14789–94. <https://doi.org/10.1073/pnas.97.26.14789>.
- Fodor J, Gullner G, Adam AL, Barna B, Komives T, Kiraly Z. Local and systemic responses of antioxidants to tobacco mosaic virus infection and to salicylic acid in tobacco (role in systemic acquired resistance). *Plant Physiol*. 1997;114(4):1443–51. <https://doi.org/10.1104/pp.114.4.1443>.
- Han CG, Li DW, Xing Y, Zhu K, Tian ZF, Cai ZN, et al. Wheat yellow mosaic virus widely occurring in wheat (*Triticum aestivum*) in China. *Plant Dis*. 2000;84(6):627–30. <https://doi.org/10.1094/PDIS.2000.84.6.627>.
- Jiang J, Patarroyo C, Cabanillas DG, Zheng HQ, Laliberté J-F. The vesicle-forming 6K2 protein of turnip mosaic virus interacts with the COPII coatomer sec24a for viral systemic infection. *J Virol*. 2015;89(13):6695–710. <https://doi.org/10.1128/JVI.00503-15>.
- Kim B, Masuta C, Matsuura H, Takahashi H, Inukai T. Veinal necrosis induced by turnip mosaic virus infection in *Arabidopsis* is a form of defense response accompanying HR-like cell death. *Mol Plant-Microbe Interact*. 2008;21(2):260–8. <https://doi.org/10.1094/MPMI-21-2-0260>.
- Kim BM, Suehiro N, Natsuaki T, Inukai T, Masuta C. The P3 protein of turnip mosaic virus can alone induce hypersensitive response-like cell death in *Arabidopsis thaliana* carrying TuNI. *Mol Plant-Microbe Interact*. 2010;23(2):144–52. <https://doi.org/10.1094/MPMI-23-2-0144>.
- Komatsu K, Hashimoto M, Ozeki J, Yamaji Y, Maejima K, Senshu H, et al. Viral-induced systemic necrosis in plants involves both programmed cell death and the inhibition of viral multiplication, which are regulated by independent pathways. *Mol Plant-Microbe Interact*. 2010;23(3):283–93. <https://doi.org/10.1094/MPMI-23-3-0283>.
- Komatsu K, Hashimoto M, Maejima K, Shiraiishi T, Neriya Y, Miura C, et al. A necrosis-inducing elicitor domain encoded by both symptomatic and asymptomatic *Plantago asiatica* mosaic virus isolates, whose expression is modulated by virus replication. *Mol Plant-Microbe Interact*. 2011;24(4):408–20. <https://doi.org/10.1094/MPMI-12-10-0279>.
- Li D, Yan L, Su N, Han C, Hou Z, Yu J, et al. The nucleotide sequence of a Chinese isolate of wheat yellow mosaic virus and its comparison with a Japanese isolate. *Arch Virol*. 1999;144(11):2201–6. <https://doi.org/10.1007/s007050050633>.
- Li HG, Shirako Y. Association of VPg and eIF4E in the host tropism at the cellular level of Barley yellow mosaic virus and wheat yellow mosaic virus in the genus *Bymovirus*. *Virology*. 2015;476:159–67. <https://doi.org/10.1016/j.virol.2014.12.010>.
- Lu YW, Yin MY, Wang XD, Chen BH, Yang X, Peng JJ, et al. The unfolded protein response and programmed cell death are induced by expression of garlic virus X p11 in *Nicotiana benthamiana*. *J Gen Virol*. 2016;97(6):1462–8. <https://doi.org/10.1099/jgv.0.000460>.
- Malcuit I, Marano MR, Kavanagh TA, Jong WD, Forsyth A, Baulcombe DC. The 25-kDa movement protein of PVX elicits Nb-mediated hypersensitive cell death in potato. *Mol Plant-Microbe Interact*. 1999;12(6):536–43. <https://doi.org/10.1094/MPMI.1999.12.6.536>.
- Mittler R, Feng X, Cohen M. Post-transcriptional suppression of cytosolic ascorbate peroxidase expression during pathogen-induced programmed cell death in tobacco. *Plant Cell*. 1998;10(3):461–73. <https://doi.org/10.1105/tpc.10.3.461>.
- Namba S, Kashiwazaki S, Lu X, Tamura M, Tsuchizaki T. Complete nucleotide sequence of wheat yellow mosaic bymovirus genomic RNAs. *Arch Virol*. 1998;143(4):631–43. <https://doi.org/10.1007/s007050050319>.
- Quevillon E, Silventoinen V, Pillai S, Harte N, Lopez R. InterProScan: protein domains identifier. *Nucleic Acids Res*. 2005;33:W116–20. <https://doi.org/10.1093/nar/gki442>.
- Schaad MC, Jensen PE, Carrington JC. Formation of plant RNA virus replication complexes on membranes: role of an endoplasmic reticulum-targeted viral protein. *EMBO J*. 1997;16(13):4049–59. <https://doi.org/10.1093/emboj/16.13.4049>.
- Sekine K-T, Ishihara T, Hase S, Kusano T, Shah J, Takahashi H. Single amino acid alterations in *Arabidopsis thaliana* RCY1 compromise resistance to cucumber mosaic virus, but differentially suppress hypersensitive response-like cell death. *Plant Mol Biol*. 2006;62(4):669–82. <https://doi.org/10.1007/s11103-006-9048-4>.
- Shevchenko AV, Budzanivska IG, Shevchenko TP, Polischuk VP, Spaar D. Plant virus infection development as affected by heavy metal stress. *Arch Phytopathol Plant Prot*. 2004;37(2):139–46. <https://doi.org/10.1080/0323540042000203967>.
- Shevchenko OV, Kamzel OA, Budzanivska IG, Shevchenko TP, Spaar D, Polischuk VP. Heavy metal soil contamination delays the appearance of virus-induced symptoms on potato but favours virus accumulation. *Arch Phytopathol Plant Prot*. 2007;40(6):406–13. <https://doi.org/10.1080/03235400600627791>.
- Soosaar JLM, Burch-Smith TM, Dinesh-Kumar SP. Mechanisms of plant resistance to viruses. *Nat Rev Microbiol*. 2005;3(10):789–98. <https://doi.org/10.1038/nrmicro1239>.
- Spetz C, Valkonen J. Potyviral 6K2 protein long-distance movement and symptom-induction functions are independent and host-specific. *Mol Plant-Microbe Interact*. 2004;17(5):502–10. <https://doi.org/10.1094/MPMI.2004.17.5.502>.
- Takeuchi T, Munekata S, Suzuki T, Senda K, Sato M. Breeding wheat lines resistant to wheat yellow mosaic virus and localization of the resistance gene (*YmMD*) derived from wheat cultivar “Madsen.” *Breed Res*. 2010;12:1–8. <https://doi.org/10.1270/jsbbr.12.1>.
- Tilsner J, Linnik O, Wright KM, Bell K, Roberts AG, Lacomme C, et al. The TGB1 movement protein of potato virus X reorganizes actin and endomembranes into the X-body, a viral replication factory. *Plant Physiol*. 2012;158(3):1359–70. <https://doi.org/10.1104/pp.111.189605>.
- Van WR, Dong X, Liu H, Tien P, Stanley J, Hong Y. Mutation of three cysteine residues in tomato yellow leaf curl virus-China C2 protein causes dysfunction in pathogenesis and posttranscriptional gene-silencing suppression. *Mol Plant-Microbe Interact*. 2002;15(3):203–8. <https://doi.org/10.1094/MPMI.2002.15.3.203>.
- Ward ER, Uknes SJ, Williams SC, Dincher SS, Wiederhold DL, Alexander DC, et al. Coordinate gene activity in response to agents that induce systemic acquired resistance. *Plant Cell*. 1991;3(10):1085–94. <https://doi.org/10.1105/tpc.3.10.1085>.
- Wei TY, Huang T-S, McNeil J, Laliberte J-F, Hong J, Nelson RS, et al. Sequential recruitment of the endoplasmic reticulum and chloroplasts for plant potyvirus replication. *J Virol*. 2010;84(2):799–809. <https://doi.org/10.1128/JVI.01824-09>.
- Wei TY, Wang AM. Biogenesis of cytoplasmic membranous vesicles for plant potyvirus replication occurs at endoplasmic reticulum exit sites in a COPI- and COPII-dependent manner. *J Virol*. 2008;82(24):12252–64. <https://doi.org/10.1128/JVI.01329-08>.
- Wei TY, Zhang C, Hou X, Sanfaçon H, Wang AM. The SNARE protein syp71 is essential for turnip mosaic virus infection by mediating fusion of virus-induced vesicles with chloroplasts. *PLoS Pathog*. 2013;9(5): e1003378. <https://doi.org/10.1371/journal.ppat.1003378>.
- Yan F, Lu YW, Lin L, Zheng HY, Chen JP. The ability of PVX p25 to form RL structures in plant cells is necessary for its function in movement, but not for its suppression of RNA silencing. *PLoS ONE*. 2012;7(8): e43242. <https://doi.org/10.1371/journal.pone.0043242>.
- Yang X, Tian YZ, Zhao X, Jiang LL, Chen Y, Hu SZ. NBALY916 is involved in potato virus X P25-triggered cell death in *Nicotiana benthamiana*. *Mol Plant Pathol*. 2020;21(11):1495–501. <https://doi.org/10.1111/mpp.12986>.
- Yoshikawa N, Saitou Y, Kitajima A, Chida T, Sasaki N, Isogai M. Interference of long-distance movement of grapevine berry inner necrosis virus in transgenic plants expressing a defective movement protein of apple chlorotic leaf spot virus. *Phytopathology*. 2006;96(4):378–85. <https://doi.org/10.1094/PHYTO-96-0378>.
- Zhan BH, Zhao WY, Li SF, Yang XL, Zhou XP. Functional scanning of apple geminivirus proteins as symptom determinants and suppressors of post-transcriptional gene silencing. *Viruses*. 2018;10(9):488. <https://doi.org/10.3390/v10090488>.

## Publisher's Note

Springer Nature remains neutral with regard to jurisdictional claims in published maps and institutional affiliations.